IEEE Access
Multidisciplinary | Rapid Review | Open Access Journal

Received October 21, 2019, accepted November 6, 2019, date of publication November 11, 2019,
date of current version November 26, 2019.

Digital Object Identifier 10.1109/ACCESS.2019.2952934

Protection of MV Closed-Loop Distribution Networks With Bi-Directional Overcurrent Relays and GOOSE Communications

BOŠTJAN POLAJŽER[1], (Member, IEEE), MATEJ PINTARIČ[1], MIRAN ROŠER[2], AND GORAZD ŠTUMBERGER[1], (Member, IEEE)

[1]Faculty of Electrical Engineering and Computer Science, University of Maribor, 2000 Maribor, Slovenia
[2]Elektro Celje, d. d., 3000 Celje, Slovenia

Corresponding author: Boštjan Polajžer (bostjan.polajzer@um.s)

This work was supported in part by the Slovenian Research Agency (ARRS) under Project P2-0115, Project L2-5489, and Project L2-7556, and in part by the Smart-Grid Project through the partnership between the Japanese Agency New Energy and Industrial Technology Development Organization (NEDO) and the Slovenian Transmission System Operator ELES, d.o.o.

ABSTRACT This paper proposes measures to improve the protection of MV distribution networks operating with feeders in a closed-loop arrangement. Bi-directional overcurrent relays (OCRs) are discussed, the selectivity of which is achieved through the timing coordination of their operation. The classic approach is formulated as a minimization of the operating times of all the OCRs. The proposed approach enhances the selectivity by considering the maximum operating time of substation OCRs and the unwanted trips of in-loop OCRs. Moreover, the sensitivity is also increased by introducing an objective function that minimizes the pickup-current settings of all the OCRs together with their operating times. Furthermore, to fulfill the demanding requirements for operating times, variable penalties are introduced. Thus, the optimization procedure is forced towards the region with viable solutions for the optimization problem. Two variants of self-adaptive differential evolution have been used that both show better convergence when compared to the classic differential evolution. Moreover, ten mutation strategies were tested, where ''rand/1/bin'' showed the best results. A comparison with other methods for timing coordination shows that the proposed optimization results in a comparable value for the OCRs' operating times. In order to further reduce the operating times, GOOSE communications between the OCRs are adopted. The proposed measures for improved protection operation are fully confirmed through dynamic simulations of the faults in the discussed 20-kV network. Moreover, the proposed protection design is already implemented and permanently operates in a 20-kV network with more than 5000 customers, whereas the field results show selective and reliable protection operation.

INDEX TERMS Closed-loop operation, overcurrent relay, selectivity, sensitivity, communications.

I. INTRODUCTION

One of the priorities of modern distribution networks is improved power-supply reliability. This is normally evaluated by the system indices SAIFI (System Average Interruption Frequency Index) and SAIDI (System Average Interruption Duration Index). A well-known solution for the improvement of system indices is fault location, isolation, and self-restoration procedures [1]. Feeders in radial or closed-loop arrangements, equipped with properly placed and adjusted protection Relays with Switching Capability (RSCs), represent another approach to improving the supply reliability. However, the key challenge in the realization of such a network operation is a proper protection system design, where all the modern solutions, such as the exchange of GOOSE (Generic Object Oriented Substation Event) messages among the relays, are applied in order to reach the goal of improved supply reliability.

The basic performance requirements for a protection relay, or a relaying system, are reliability, sensitivity, selectivity and fault-clearing time [2], [3]. The selectivity of overcurrent relays (OCRs) is achieved by the timing coordination of their operation. This can be performed using different optimization approaches [4]–[17]. In [4] an interval linear

The associate editor coordinating the review of this manuscript and approving it for publication was Md Shihanur Rahman.

programming problem was formulated, considering changes in the network topologies. A seeker algorithm was proposed in [5] to solve a mixed-integer nonlinear programming (MINLP) problem. The complexity of the non-linear programing problem was reduced in [6] through reformulation as an equivalent, quadratically constrained, quadratic programming (QCQP) model. In [7] a local-fit method was proposed by defining reference marks based on the OCR's characteristics. Furthermore, several metaheuristic algorithms were applied, like enhanced differential evolution [8], a combination of the differential evolution and linear programming problem [9], a genetic algorithm [10], a combination of the genetic algorithm and the linear programming problem [11], or a combination of a specialized genetic algorithm and an efficient heuristic algorithm [12]. Moreover, a symbiotic organism search algorithm [13], teaching learning-based optimization [14], particle-swarm optimization [15], ant-colony optimization [16], and whale optimization algorithm [17] were also applied. Lately, distributed generation (DG) was also considered within the timing coordination of the OCR's operation [18]–[21].

The timing coordination inherently introduces a time delay to the OCRs' operation, which can be improved using a peer-to-peer communication by applying GOOSE messages [22], [23]. Typically, the GOOSE-based communication is used in substation-area protection [24], [25]; however, inter-substation communication was already applied, e.g., for accelerated distance-protection operation [26]. When using a proper communication network, GOOSE messages can also be sent between all the OCRs in a MV distribution network. The required reliability and security of GOOSE messages can be achieved using recovery protocols [27] as well as digital signature algorithms [28].

The organization of the paper is as follows. In Section II, the background to the parametrization of bi-directional OCRs is presented. Section III proposes measures for the improved operation of bi-directional OCRs. The sensitivity is increased by minimizing the pickup-current settings, together with the operating times, which is an original contribution of this paper. Furthermore, a simple approach is proposed to avoid unwanted trips of the in-loop OCRs. Moreover, the selectivity of the substation OCRs is achieved by limiting their operating times, which is not discussed in the literature. A self-adaptive differential evolution (SADE) algorithm [29] is applied to minimize the operating times and the pickup-current settings of all the OCRs, while introducing variable penalties. In order to further reduce the operating times of the OCRs, a peer-to-peer communication is proposed, according to the GOOSE model. The proposed methodology for the parametrization of the OCRs is given and validated in Section IV.

In order to confirm the discussed measures for the improved protection operation, a case study is considered in Section V. A 20-kV network with three possible network topologies (two different loops and a radial type) that is equipped with properly placed bi-directional RSCs with

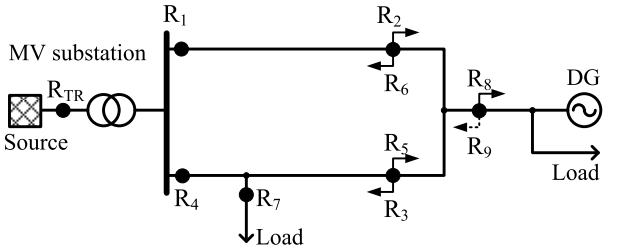

Relay pairs (primary, back-up): $(R_2,R_1)_1$, $(R_3,R_2)_2$, $(R_3,R_9)_3$, $(R_5,R_4)_4$, $(R_6,R_5)_5$, $(R_6,R_9)_6$, $(R_7,R_4)_7$, $(R_7,R_3)_8$, $(R_8,R_2)_9$, $(R_8,R_5)_{10}$

FIGURE 1. Illustrative example with relay pairs.

GOOSE communications is discussed. The parameterization of the RSCs and substation OCRs was performed according to the proposed methodology. Furthermore, a detailed network model was built, together with a dynamic model of the discussed RSC and GOOSE communications, which is not reported in the literature. The results are given in Section VI. First, two different SADE variants and ten mutation strategies are analyzed through the best objective function value and the convergence. Next, the selectivity is tested using theoretical calculations of the operating times of the primary and back-up OCRs. Furthermore, based on dynamic simulations of the faults, the fault-clearing times are given for all the RSCs and substation OCRs, which is not discussed in the literature. Moreover, a comparison is also made for a protection system with and without GOOSE-based communications. The proposed protection design has already been implemented and since January 2019 has been in permanent operation in a 20-kV network of Distribution Company (DisCo) Elektro Celje with more than 5000 customers, which represents an additional contribution of this paper. Section VII concludes the paper.

II. BACKGROUND

A. RELAY NOTATION AND RELAY PAIRS

Most of the research about the timing coordination of the operation of OCRs assumes that the OCRs are located at the network's buses, which is not feasible in MV distribution networks. The OCRs are located at the substation feeders, whereas along the feeders the RSCs are mounted directly on a tower construction. Furthermore, MV distribution networks can also operate in a closed-loop, whereas between two successive OCRs there might be a considerable in-feed due to the DG. One of the most favorable protection solutions is the bi-directional OCR [18].

An arbitrary relay notation will be used, as shown in Fig. 1 for an illustrative example. Note that an individual bi-directional relay is separately denoted for each direction, e.g., R_2, R_6. Furthermore, the relays located at substation R_1 and R_4 are non-directional, as well as R_7, since no source is assumed on that side branch. Moreover, the incorporation of R_9 depends on the DG capacity, which should be checked using short-circuit calculations.

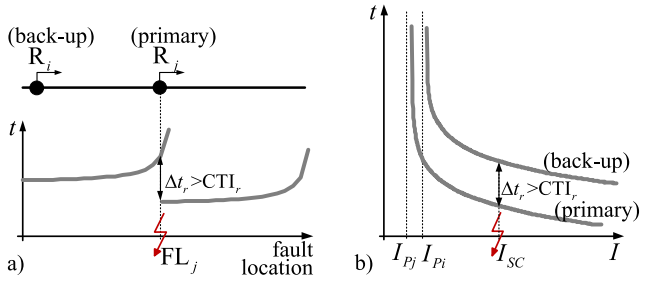

FIGURE 2. Timing coordination for a fundamental relay pair $(R_j, R_i)_r$: time-fault location characteristics (a), and time-current characteristics (b).

In order to achieve the timing coordination of the OCRs' operation, relay pairs should be determined. An individual relay pair consists of a primary and a back-up OCR. The following notation will be used for the r-th relay pair, i.e., $(R_j, R_i)_r$, where R_j and R_i, respectively, denote the primary and back-up OCRs. The relay pairs for the discussed example are given in Fig. 1. Note that the relay pairs $(R_3, R_9)_3$ and $(R_6, R_9)_6$ might not be necessary, depending on the DG's capacity. Furthermore, the transformer relay R_{TR} is not considered in the timing coordination through relay pairs, since its settings are fixed and predefined. Moreover, a definite time-current characteristic is typically used for the relay R_{TR}, while other relays use an inverse time-current characteristic. Therefore, the timing coordination is achieved by limiting the operating times of the relays R_1 and R_4, i.e., they should operate faster than the relay R_{TR}.

B. TIME-CURRENT CHARACTERISTICS

Different types of time-current characteristics can be used, i.e., definite-time, inverse-time or custom-based, e.g., piecewise linear [31]. In the following, only the inverse-time characteristic will be discussed, which is given as

$$t_{j,k} = T_{Dj}\left(\frac{A}{\left(\frac{I_{j,k}}{I_{Pj}}\right)^{B} - 1} + C\right) \tag{1}$$

where $t_{j,k}$ and $I_{j,k}$ denote the operating time and the current passing through the j-th OCR for a fault at location FL_k. I_{Pj} and T_{Dj} denote the pickup-current setting and the time-dial setting, respectively. The constants A, B and C are given according to the characteristic type, which is defined by the IEC [32] or IEEE [33] standards.

The notation introduced in (1) refers to a j-th OCR and a fault at location FL_k. However, when considering an r-th relay pair, then the notation $(\cdot)_{(p,r)}$ and $(\cdot)_{(b,r)}$ will refer to the primary and back-up OCRs, respectively, while considering the fault location at a primary OCR (Fig. 2a).

C. PICKUP-CURRENT LIMITS

In order to ensure the reliable operation of an OCR, the pickup current should be greater than the maximum-possible load current and lower than the minimum short-circuit current with a reasonable security margin. Furthermore, the measurement error of the used current transformers (CTs) should also be considered. Thus, the pickup-current limits of the j-th OCR can be determined as

$$\begin{aligned} I_{Pj\,\min} &> \left(1 + K_L \frac{e_{\mathrm{CT}\%}}{100}\right) I_{j,L\,\max} \\ I_{Pj\,\max} &< \left(1 - K_{SC} \frac{e_{\mathrm{CT}\%}}{100}\right) I_{j,SC\,\min} \end{aligned} \tag{2}$$

where $I_{j,SC\,\min}$ is the minimum short-circuit current, i.e., for a Phase-to-Phase (Ph-Ph) fault located at a remote end of the discussed line. $I_{j,L\,\max}$ is the maximum value of the transient load current. Furthermore, $e_{\mathrm{CT}\%}$ denotes the % measurement error of the used CTs, whereas $K_{SC} > 1$ and $K_L > 1$ are security factors [34].

D. TIMING COORDINATION

Selectivity is achieved by timing coordination, where the OCR intended to operate (primary) operates faster than the other OCRs (back-up), as shown in Fig. 2. Selectivity is ensured when $\Delta t_r > \mathrm{CTI}_r$, where $\Delta t_r = (t_{(b,r)} - t_{(p,r)})$. CTI_r is a coordination time interval that is determined according to the specified time delays of both OCRs and the operating times of the switch gears.

The pickup-current settings and the time-dial settings of all the OCRs can be determined in different ways [4]–[17]. The classic approach is formulated as a minimization of an objective function that is given as a sum of the operating times of all the primary and back-up OCRs, i.e.,

$$T = \sum_{r=1}^{N_{RP}} \left(t_{(p,r)} + t_{(b,r)}\right) + p \tag{3}$$

where N_{RP} is the number of all the relay pairs. The operating times $t_{(p,r)}$ and $t_{(b,r)}$ should be calculated using (1), where currents that correspond to the fault location given by the primary OCRs should be used (Fig. 2a). Note that short-circuit currents passing through the primary and back-up relays have the same magnitude only for the fundamental relay pair, which is in Fig. 2b denoted by I_{SC}. However, in the case of a side branch between both relays, e.g., R_5 and R_4 in Fig. 1, the magnitude of the currents passing through both relays will not be equal. The penalties p are generally applied when $\Delta t_r \leq \mathrm{CTI}_r$, or when violating the limits of the pickup-current or time-dial settings. Moreover, penalties should also be applied when the operating times of substation OCRs, such as R_1 and R_4 in Fig. 1, exceed a permissible value given by the operating time of the relay R_{TR}.

E. COMMUNICATIONS

The operating times of the OCRs can be considerably reduced using the communications between the OCRs. Generally, two different communication schemes can be used, i.e., release or block [35]. They are shown in Fig. 3 for a line supplied from both ends. When using the release scheme (Fig. 3a) then each OCR that picks-up according to the direction criterion releases its neighboring OCR in the

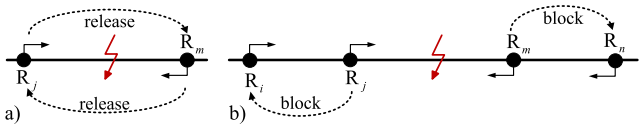

FIGURE 3. Communications between OCRs on a line supplied from both ends: release (a), and block (b).

direction of the fault. Furthermore, when using the block scheme (Fig. 3b), then each OCR that picks-up according to the direction criterion blocks its neighboring OCR in the opposite direction of the fault. However, in cases of communication failure or delay in communications the operation of the OCRs should meet the performance requirements on reliability, sensitivity and selectivity.

III. MEASURES TO IMPROVE AN OCR'S OPERATION IN MV CLOSED-LOOP DISTRIBUTION NETWORKS

A. INCREASING SENSITIVITY

The pickup-current setting I_{Pj} can be chosen within the limits given by (2). A high setting of I_{Pj} will inherently reduce the sensitivity. Consequently, high-resistance faults might not be ''seen'' by the j-th OCR, or its operating time might be delayed due to the inverse time-current characteristic. It is, therefore, preferable to set I_{Pj} as low as possible; moreover, a low setting of I_{Pj} will also reduce the operating time. However, low settings of I_{Pj} must not affect the selectivity. This can be achieved through a simultaneous minimization of the OCRs' operating times and pickup-current settings. Thus, a normalized objective function is proposed as

$$q = \alpha \frac{1}{N_{RP}} \sum_{r=1}^{N_{RP}} \frac{t_{(p,r)} + t_{(b,r)}}{t_{EV}} + \beta \left(1 + \frac{1}{N_R} \sum_{j=1}^{N_R} \frac{I_{Pj} - I_{Pj\min}}{I_{Pj\max} - I_{Pj\min}} \right) + p \quad (4)$$

where α and β are the weights ($\alpha + \beta \leq 1$), whereas N_{RP} and N_R denote the number of relay pairs and the number of OCRs, respectively. The first term in (4) represents the mean value of the operating times of all the primary and back-up OCRs normalized to the expected value t_{EV}. The second term represents the mean value of the pickup-current settings, which are normalized using a min-max approach.

B. ENHANCING SELECTIVITY

Selectivity is achieved by the timing coordination of the OCR's operation, as described in Section II-D, i.e., by fulfilling the condition $\Delta t_r > \mathrm{CTI}_r$ for the r-th relay pair. In order to enhance the selectivity of the OCRs in MV distribution networks, the following topics should be addressed.

1) INVERSE TIME-CURRENT CHARACTERISTIC TYPE

The timing coordination of the OCRs in MV distribution networks faces two competing factors. One factor is the large number of relays along the feeder, loop or a side branch. Another is the maximum permissible operating times of substation OCRs, like R_1 and R_4 in Fig. 1. In order to enhance the selectivity, an extremely inverse characteristic is proposed.

2) AVOIDING UNWANTED TRIPS OF IN-LOOP OCRS

Generally, unwanted trips occur due to the changes in topology, location or level of the fault. Such situations are possible for in-loop OCRs, i.e., when the current flowing through a designated relay pair is increased due to the faster operation of the remote OCR in the direction of a fault. Let us consider a fault in a section between R_2 and R_5 (Fig. 1). When R_5 and R_9 operate first, then the current flowing through R_2 and R_1 will increase, which will result in a decreased Δt between R_2 and R_1. Consequently, R_1 might operate faster than R_2. In order to avoid such unwanted trips the short-circuit calculations should be performed for two different states, defined by the operation of the in-loop OCRs. The first state is given by the normal loop topology. The second state considers the changed topology, i.e., the loop is opened at the location of a remote OCR in the direction of a fault. The largest value between the so-obtained currents is then used for the timing coordination of the designated relay pair, i.e., $(R_2, R_1)_1$ in the discussed case (Fig. 1). This simple procedure increases the selectivity and reliability.

3) SUBSTATION OCRs

The selectivity of the substation OCRs (R_1 and R_4 in Fig. 1) is achieved through a timing coordination with the transformer relay R_{TR}. Typically, an OCR with a definite time characteristic is used for the relay R_{TR}, where the pickup current is set for a fault at the beginning of the feeder. Consequently, the selectivity of the j-th substation OCR is achieved by limiting its operating time for a fault at the beginning of the feeder, which is denoted as $t^*_{j,k}$. The typical limit for MV networks is given as $t^*_{j,k} < 300$ ms.

C. OPTIMIZATION

1) SELF-ADAPTIVE DIFFERENTIAL EVOLUTION

A stochastic search algorithm called differential evolution (DE), capable of solving nonlinear and bounded optimization problems, has been applied as an optimization tool [30]. It has been chosen because of its simplicity and proven suitability for solving real-life engineering problems. DE incorporates a scheme that generates trial parameter vectors, which involves three operations: mutation, crossover, and selection. There are several mutation strategies; however, the best strategy for solving a particular optimization problem depends on the problem itself. The control parameters of the DE algorithm are the population size NP, the step size F and the crossover-probability constant CR. The suggested choices of [30] are $F \in [0.5, 1]$, $CR \in [0.8, 1]$, and $NP = 10D$. Here, D denotes a dimension of a parameter vector. In the given case $D = 2\,N_R$, since the j-th OCR has two setting parameters, i.e., I_{Pj} and T_{Dj}. Furthermore, choosing suitable values for F and CR is a

problem-dependent task. Therefore, self-adaptive differential evolution (SADE) has been used, where F and CR are adapted as proposed in [29]. Note that when using a classic DE, then approximately one million iterations were needed for the case study discussed in this paper, whereas when using SADE the number of iterations was considerably reduced.

2) VARIABLE PENALTIES

A very important part of the performed optimization is the penalties p in the objective function (4). Note that when using fixed penalties the optimization process was not converging for the case study discussed in this paper. Therefore, the penalties were introduced in such a way that they force the optimization procedure towards the region with viable solutions of the optimization problem. This means that the penalties are dependent on the difference between the actual values of the individual parameters, and their minimum- or maximum-allowed values, thus ensuring the convergence of the optimization procedure.

The penalties are calculated for $\Delta t_r \leq \mathrm{CTI}_r$ (typical CTI value is within the range 100 to 300 ms), $t^*_{j,k} \geq 300$ ms, $T_{Dj} < T_{Dj\,\mathrm{min}}$, $I_{Pj} < I_{Pj\,\mathrm{min}}$ and $I_{Pj} > I_{Pj\,\mathrm{max}}$. For all the aforementioned parameters ($\Delta t_r, t^*_{j,k}, T_{Dj}, I_{Pj}$), the values for which V are bounded with the minimum V_{min} and the maximum V_{max} allowed values, the variable penalties p_V are introduced according to the pseudo code:

if $V < V_{\mathrm{min}}$ **then**
  $p_V = ((|V_{\mathrm{min}} - V| + 1)K_1)^{K_2}$
end if
if $V > V_{\mathrm{max}}$ **then**
  $p_V = ((|V - V_{\mathrm{max}}| + 1)K_1)^{K_2}$
end if

where $K_1 = 10$ and $K_2 = 4$ are the constants, the values of which were determined based on experiences. The values of all the penalties p_V determined in this way for all relay pairs are summed up and added as a penalty p in (4). The described procedure forces (4) to fulfill all the optimization bounds before the actual operating times and pickup-current settings are minimized. The authors are not aware of a publication where the proposed approach is applied to the operating-time minimization of OCRs that provides the required selectivity and sensitivity in a MV closed-loop distribution network.

D. PEER-TO-PEER COMMUNICATIONS

The IEC standard 61850 [22] enables peer-to-peer communications between different devices. Protection applications require high-speed peer-to-peer-communications that should guarantee the total transfer time below the order of a quarter of a cycle. GOOSE messages have the shortest maximum-allowed transfer time among all the IEC 61850 messages, corresponding to the required 3 ms. They can be sent over TCP/IP or substation local area networks using high-speed switched Ethernet. Furthermore, the exchange of GOOSE messages between devices is based on a publisher-subscriber mechanism. This allows, e.g., the OCR to deliver the information simultaneously to a predefined group of destination OCRs.

In the given case the pick-up GOOSE messages will be sent between the RSCs and the substation OCRs. However, an instantaneous trip will be enabled only when the OCR receives the message and when the condition given by a logical equation is fulfilled. Thus, e.g., the instantaneous trip of R_3 and R_4 shown in Fig. 1 should be enabled only when they receive a pick-up message from each other, and when they do not receive a pick-up message from R_7. In this way the faults on the line between R_3 and R_4 can be cleared faster, whereas for the faults on the side branch only R_7 will operate according to the set time-current characteristic.

IV. METHODOLOGY FOR THE PARAMETERIZATION OF OCRS

This section summarizes the proposed measures for improving the OCRs' operation in MV distribution networks. Thus, a methodology for the parameterization of OCRs is given by the following steps:

- Step 1: Relay points are determined that require bi-directional OCRs. In cases where larger DGs are connected, the short-circuit calculations are needed to check their impact on the current directions (R_9 in Fig. 1).
- Step 2: Short-circuit calculations are performed for Ph-Ph faults at all the relay points, as well as at the ends of all the lines. For all the in-loop relays, short-circuit calculations should be performed for two different states (Section III-B2).
- Step 3: Pickup-current limits are determined for all the OCRs (Section II-C).
- Step 4: Pickup-current settings and time-dial settings are determined through the minimization of the proposed objective function using the SADE algorithm and the mutation strategy "rand/1/bin" (Sections III-A and III-C).
- Step 5: Communications are applied according to the GOOSE model, where a release communication scheme is adopted for all the in-loop OCRs (Sections II-E and III-D).

The proposed timing coordination is validated for a three-bus system through a comparison with the MINLP using a standard branch-and-bound (SBB) and a seeker algorithm [5], and through the comparison with the QCQP-based algorithm [6]. To make a clear comparison the same assumptions and limits were used as in [5], [6], i.e., I_{Pj} and T_{Dj} were limited to the minimum values of 1.5 A (secondary) and 100 ms, respectively, whereas the IEC standard inverse characteristic was used. Furthermore, one-directional OCRs were used, and thus the relay pairs were defined as in Fig. 4. Note that timing coordination with the protection relays of the generators G_1, G_2 and G_3 was not considered. Moreover, $\mathrm{CTI}_r = 0.2$ s was used when comparing the results with [5], whereas $\mathrm{CTI}_r = 0.3$ s was used when comparing the results with [6]. The objective function (4) was minimized, where

TABLE 1. Relay settings for the three-bus system – IEC Standard Inverse ($A = 0.14, B = 0.02, C = 0$).

	CTI$_r$= 0.2 s						CTI$_r$ =0.3 s			
	SBB [5]		Seeker [5]		DE–Proposed		QCQP [6]		DE–Proposed	
	I_{Pj} [A]	T_{Dj} [ms]	I_{Pj} [A]	T_{Dj} [ms]	I_{Pj} [A]	T_{Dj} [ms]	I_{Pj} [A]	T_{Dj} [ms]	I_{Pj} [A]	T_{Dj} [ms]
R_1	1.5	151	2.5	107	1.958	100	2.862	100	2.863	100
R_2	2.0	100	1.5	112	1.500	100	1.720	100	1.720	100
R_3	1.5	128	2.0	108	1.500	100	1.500	100	1.500	100
R_4	2.0	130	3.0	100	1.795	100	2.482	100	2.482	100
R_5	2.5	106	2.5	100	1.500	100	1.500	100	1.500	100
R_6	2.5	104	2.5	100	1.690	100	2.342	100	2.323	100
T [s]	6.362		6.324		4.534		5.032		5.033	
T' [s]	6.403		6.359		4.550		5.031		5.027	

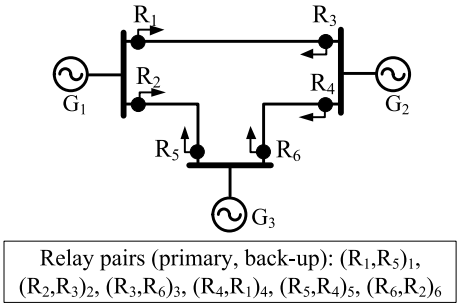

FIGURE 4. The three-bus system with relay pairs.

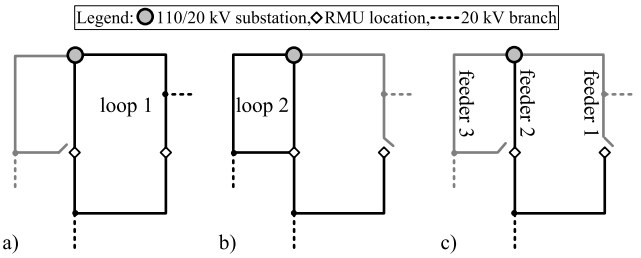

FIGURE 5. Discussed topologies of a 20-kV network: Loop 1 (a), Loop 2 (b), and Radial (c), where RMU is a Ring Main Unit.

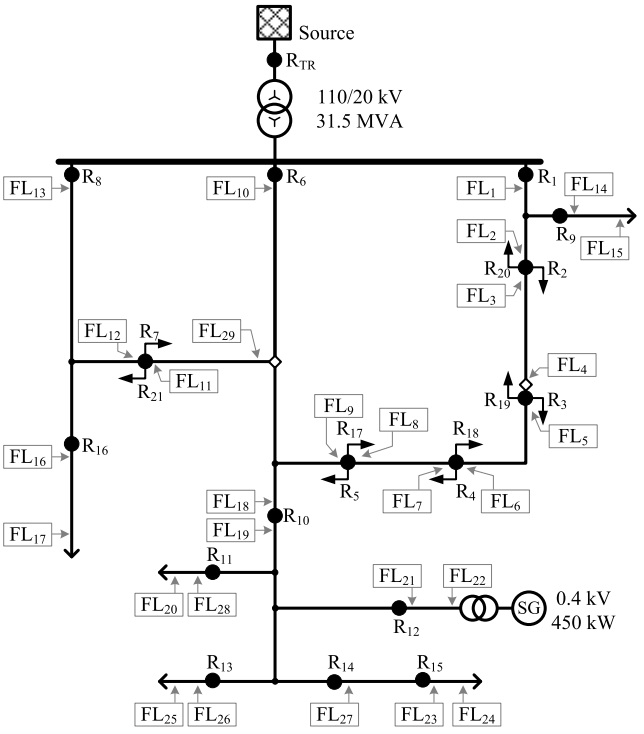

FIGURE 6. Discussed 20-kV network with denoted OCRs and fault locations.

$\alpha = 0.3$, $\beta = 0.7$ and $t_{EV} = 0.3$ s. The obtained settings of the OCRs are given in Table 1 together with the value of T. Note that these settings cannot be applied. Therefore, the value of T' is also given for the settings rounded to 10 mA (secondary) and 10 ms. The proposed timing coordination gives a better value of T and T' when compared to the SBB and seeker algorithms, whereas the difference with the result obtained using the QCQP-based algorithm is negligible. Furthermore, a comparison with a recent paper [17] was also made, where only the value for $\sum t_{(p,r)}$ is given, i.e., 1.526 s. The result obtained using the proposed timing coordination was 1.513 s.

V. CASE STUDY

A 20-kV network of DisCo Elektro Celje is discussed. Three feeders, connected to a 110/20-kV transformer substation, supply altogether 109 MV/LV distribution transformers with over 5000 customers, along with 30 DG units. The entire 20-kV network contains 296 nodes and 297 branches, forming two loops that can be remotely opened or closed by ring main units (RMUs). Furthermore, compact RSCs [36] are used at 13 relay points that were determined by the DisCo, whereas ordinary OCRs are adopted at the substation. Moreover, all the OCRs enable GOOSE communications.

A. DISCUSSED NETWORK TOPOLOGIES

Fig. 5 shows three network topologies, i.e., Loop 1, Loop 2 and Radial, that will be further discussed. The entire 20-kV network is shown in Fig. 6. Only a small hydro-power plant with a synchronous generator (SG) is shown, whereas other DGs are micro solar power plants and are not considered because of their negligible contribution to the fault currents. Relay pairs, fault locations, as well as communication pairs are given in this section for all three network topologies.

1) RELAY PAIRS AND UNWANTED TRIPS

Protection is applied at 16 relay locations, as shown in Fig. 6. The relays are numbered R_1 to R_{21}, whereas the fault

TABLE 2. Relay pairs (∗ denotes substation OCR) for all three network topologies with fault locations used for timing coordination.

Loop 1		Loop 2		Radial	
$(R_2,R_1^*)_1$	FL_3	$(R_2,R_1^*)_1$	FL_3	$(R_2,R_1^*)_1$	FL_3
$(R_3,R_2)_2$	FL_5	$(R_{17},R_6)_2$	FL_8	$(R_9,R_1^*)_2$	FL_{14}
$(R_4,R_3)_3$	FL_7	$(R_{17},R_7)_3$	FL_8	$(R_{17},R_6^*)_3$	FL_8
$(R_5,R_4)_4$	FL_9	$(R_{18},R_{17})_4$	FL_6	$(R_{18},R_{17})_4$	FL_6
$(R_{17},R_6^*)_5$	FL_8	$(R_7,R_8^*)_5$	FL_{11}	$(R_{10},R_6^*)_5$	FL_{19}
$(R_{18},R_{17})_6$	FL_6	$(R_{21},R_6^*)_6$	FL_{12}	$(R_{11},R_{10})_6$	FL_{28}
$(R_{19},R_{18})_7$	FL_4	$(R_9,R_1^*)_7$	FL_{14}	$(R_{12},R_{10})_7$	FL_{21}
$(R_{20},R_{19})_8$	FL_2	$(R_{10},R_7)_8$	FL_{19}	$(R_{13},R_{10})_8$	FL_{26}
$(R_7,R_8^*)_9$	FL_{11}	$(R_{10},R_6^*)_9$	FL_{19}	$(R_{14},R_{10})_9$	FL_{27}
$(R_9,R_1^*)_{10}$	FL_{14}	$(R_{11},R_{10})_{10}$	FL_{28}	$(R_{15},R_{14})_{10}$	FL_{23}
$(R_9,R_{20})_{11}$	FL_{14}	$(R_{12},R_{10})_{11}$	FL_{21}	$(R_7,R_8^*)_{11}$	FL_{11}
$(R_{10},R_5)_{12}$	FL_{19}	$(R_{13},R_{10})_{12}$	FL_{26}	$(R_{16},R_8^*)_{12}$	FL_{16}
$(R_{10},R_6^*)_{13}$	FL_{19}	$(R_{14},R_{10})_{13}$	FL_{27}	–	–
$(R_{11},R_{10})_{14}$	FL_{28}	$(R_{15},R_{14})_{14}$	FL_{23}	–	–
$(R_{12},R_{10})_{15}$	FL_{21}	$(R_{16},R_8^*)_{15}$	FL_{16}	–	–
$(R_{13},R_{10})_{16}$	FL_{26}	$(R_{16},R_{21})_{16}$	FL_{16}	–	–
$(R_{14},R_{10})_{17}$	FL_{27}	–	–	–	–
$(R_{15},R_{14})_{18}$	FL_{23}	–	–	–	–
$(R_{16},R_8^*)_{19}$	FL_{16}	–	–	–	–

TABLE 3. Relay pairs with relay locations (RL) where a loop should be opened to avoid in-loop unwanted trips.

Loop 1		Loop 2	
$(R_2,R_1)_1$	RL_3	$(R_7,R_8)_5$	RL_6
$(R_3,R_2)_2$	RL_4	$(R_{21},R_6)_6$	RL_8
$(R_4,R_3)_3$	RL_5	–	–
$(R_5,R_4)_4$	RL_6	–	–
$(R_{17},R_6)_5$	RL_4	–	–
$(R_{18},R_{17})_6$	RL_3	–	–
$(R_{19},R_{18})_7$	RL_2	–	–
$(R_{20},R_{19})_8$	RL_1	–	–

Note: RL_x corresponds to the location of a relay R_x.

locations are denoted as FL_1 to FL_{29}. All the in-loop OCRs, except the substation relays R_1, R_6 and R_8, are bi-directional. Furthermore, R_{12} and R_{10} are non-directional, since a small SG does not change the fault current directions. Relay pairs are given in Table 2. Moreover, relay locations at which a loop should be opened to avoid unwanted trips are given in Table 3, as proposed in Section III-B2.

2) FAULT LOCATIONS

In order to perform the timing coordination of the OCRs, the fault locations were determined according to the rule given in Section II-D. They are given in Table 2, together with the relay pairs. Furthermore, in order to determine the maximum pickup-current limits, the fault locations were determined according to the rule given in Section II-C. They are given in Table 4, where $FL_{x,y}$ denotes two possible fault locations, i.e., FL_x and FL_y. In such cases only a fault location that results in a smaller current measured by the corresponding OCR is considered. However, the considered current value should be larger than the maximum load current.

3) GOOSE-BASED COMMUNICATIONS

Table 5 shows the subscriptions of all the OCRs to the GOOSE messages sent by the other OCRs. The logical

TABLE 4. Relays for all three network topologies with fault locations used for the determination of the pickup-current limits.

Loop 1		Loop 2		Radial	
R_1	$FL_{2,14}$	R_1	$FL_{2,14}$	R_1	$FL_{2,14}$
R_2	FL_4	R_2	FL_4	R_2	FL_4
R_3	FL_6	–	–	–	–
R_4	FL_8	–	–	–	–
R_5	$FL_{18,10}$	–	–	–	–
R_6	$FL_{9,18}$	R_6	$FL_{9,18,11}$	R_6	$FL_{9,18}$
R_7	FL_{29}	R_7	$FL_{10,9,18}$	R_7	FL_{29}
R_8	$FL_{12,16}$	R_8	$FL_{12,16}$	R_8	$FL_{12,16}$
R_9	FL_{15}	R_9	FL_{15}	R_9	FL_{15}
R_{10}	$FL_{28,21,26,27}$	R_{10}	$FL_{28,21,26,27}$	R_{10}	$FL_{28,21,26,27}$
R_{11}	FL_{20}	R_{11}	FL_{20}	R_{11}	FL_{20}
R_{12}	FL_{22}	R_{12}	FL_{22}	R_{12}	FL_{22}
R_{13}	FL_{25}	R_{13}	FL_{25}	R_{13}	FL_{25}
R_{14}	FL_{23}	R_{14}	FL_{23}	R_{14}	FL_{23}
R_{15}	FL_{24}	R_{15}	FL_{24}	R_{15}	FL_{24}
R_{16}	FL_{17}	R_{16}	FL_{17}	R_{16}	FL_{17}
R_{17}	FL_7	R_{17}	FL_7	R_{17}	FL_7
R_{18}	FL_5	R_{18}	FL_5	R_{18}	FL_5
R_{19}	FL_3	–	–	–	–
R_{20}	$FL_{1,14}$	–	–	–	–
–	–	R_{21}	$FL_{13,16}$	–	–

TABLE 5. GOOSE message subscriptions and logic equations.

	Subscribed to GOOSE message send by	Logical equation for instantaneous trip
R_1	R_{20}, R_9	$y_1 \cdot x_{20} \cdot \bar{x}_9$
R_2	R_{19}	$y_2 \cdot x_{19}$
R_3	R_{18}	$y_3 \cdot x_{18}$
R_4	R_{17}	$y_4 \cdot x_{17}$
R_5	R_6, R_{10}	$y_5 \cdot x_6 \cdot \bar{x}_{10}$
R_6	R_5, R_7, R_{10}	$y_6 \cdot (x_5 + x_7) \cdot \bar{x}_{10}$
R_7	R_6, R_{10}	$y_7 \cdot x_6 \cdot \bar{x}_{10}$
R_8	R_{21}, R_{16}	$y_8 \cdot x_{21} \cdot \bar{x}_{16}$
R_9	–	–
R_{10}	R_{11}, R_{12}, R_{13}, R_{14}	$y_{10} \cdot \bar{x}_{11} \cdot \bar{x}_{12} \cdot \bar{x}_{13} \cdot \bar{x}_{14}$
R_{11}	–	–
R_{12}	–	–
R_{13}	–	–
R_{14}	R_{15}	$y_{14} \cdot \bar{x}_{15}$
R_{15}	–	–
R_{16}	–	–
R_{17}	R_4	$y_{17} \cdot x_4$
R_{18}	R_3	$y_{18} \cdot x_3$
R_{19}	R_2	$y_{19} \cdot x_2$
R_{20}	R_1, R_9	$y_{20} \cdot x_1 \cdot \bar{x}_9$
R_{21}	R_8, R_{16}	$y_{21} \cdot x_8 \cdot \bar{x}_{16}$

Legend: $y_j \ldots$ local pick-up, $x_i \ldots$ received pick-up message, $\bar{x}_i \ldots$ not received pick-up message, "·" logical AND, "+" logical OR.

equations that should be fulfilled for starting an instantaneous trip that is based on received pick-up GOOSE messages x_i and the local pick-up y_j are also given. Pick-up GOOSE messages are sent between the neighboring in-loop OCRs, while the OCRs on the side branches are also included to achieve selectivity, e.g., R_1 is subscribed to the messages sent by R_{20} and R_9. For the discussed case the instantaneous trip of R_1 is possible when receiving a pick-up message from R_{20} and not receiving it from R_9, which is denoted in Table 5 as $y_1 \cdot x_{20} \cdot \bar{x}_9$. Furthermore, the operating time of R_{10} can also be decreased, i.e., when not receiving the pick-up message from one of R_{11}, R_{12}, R_{13}, R_{14}. The operating time of R_{14} can be

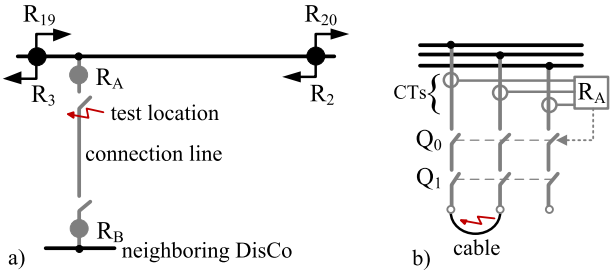

FIGURE 7. Field testing on a section between relays R_{19} and R_2: test location (a) and a Ph-Ph fault (b).

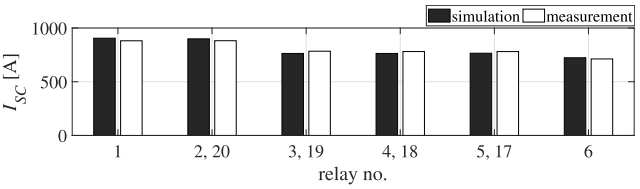

FIGURE 8. Measured and simulated rms values of short-circuit currents during a Ph-Ph test for relays in Loop 1, where bi-directional relays are denoted by two numbers.

decreased in a similar way, i.e., when not receiving the pick-up message from R_{15}. Note that in cases of communication failure or delay in communications the OCRs should operate according to the set time-current characteristic.

B. MODELING

The model of the discussed 20-kV network and the model of a bi-directional RSC were both built for MATLAB/Simulink/Simscape Power Systems. It should be pointed out that they were verified through extensive laboratory and field testing.

1) NETWORK MODEL

A 110-kV source was modeled as a constant impedance with a maximum short-circuit capacity of 6.679 kA. Furthermore, the discussed 20-kV network incorporates π models of underground cables and overhead lines, as well as generic models of transformers and a SG. According to the measured load and generating profiles for a period of 15 months a maximum load was determined for all the MV/LV transformer locations. Thus, a constant power-load model was incorporated on the LV side of each corresponding transformer. The developed 20-kV network model can be used for static short-circuit calculations as well as for dynamic simulations of the relay operation. The step size for the dynamic simulations was set to 0.0625 ms, whereas a step size of 2.5 ms was used for the calculation of the phasors.

Field testing was performed to verify the discussed MV network model. A Ph-Ph fault was generated in a controlled way, where special care was taken not to disconnect any customers. The fault was located near R_{19}, i.e., at the beginning of a line that can be used to connect the discussed network to a network of the neighboring DisCo, as shown in Fig. 7a. During normal operation this line is only connected from side A; however, it can be connected from both sides in cases of a total power loss in one of the DisCos. Note that an OCR is located on both sides of the line, i.e., R_A and R_B. During the test, the discussed line was connected only from side A. No special equipment was needed to perform the test, except a cable used for the Ph-Ph connection, as shown in Fig. 7b. Only the Loop-1 topology was tested, while the following procedure was followed:

Step 1: All the in-loop relays were set only to pick-up without operation, whereas the relay R_A was set to pick-up and operate with no delay.

Step 2: Switch gear Q_1 was closed first, then the closed poles were visually inspected.

Step 3: Switch gear Q_0 was closed next to generate a Ph-Ph fault.

Step 4: Relay R_A operated, and Q_0 was opened after approximately 60 ms. Note that none of the customers were disconnected.

All the relays in the Loop 1 picked-up without operation and recorded the time responses of the line currents. Note that the directional criterion was not activated during the test. Furthermore, the distance between the test location and R_{19} is 0.6 km. Since the length of the section between R_{19} and R_2 is 10.9 km, the fault location FL_4 was assumed when comparing the field testing and simulation results. The comparison of the measured and simulated rms values of the currents is shown in Fig. 8, where the simulated values agree with the measured ones within a range of $\pm 3\%$.

2) BI-DIRECTIONAL RSC MODEL

A generic model of a switch gear was used with a specified time delay of 50 ms. Furthermore, a dynamic model of a bi-directional overcurrent function was built according to the specifications given by the manufacturer [36]. It is composed of the following units. The model of the input unit incorporates filtering and sampling. The line currents and voltages are filtered by low-pass, second-order Butterworth filters with a cut-off frequency of 1.6 kHz, while the sampling frequency is 3.2 kHz. Next, a discrete Fourier filtering is applied using a full-cycle data-window. The resulting phasors are refreshed every 2.5 ms. The model of the main unit describes the overcurrent function with IEC inverse-time pickup characteristics and additional definite-time reset characteristics. Furthermore, a bi-directional functionality was modeled with a standard directional criterion, which is based on the angle between the current phasor and the line-voltage phasor. The model of the logic unit provides the pickup and trip signals. Moreover, a GOOSE model was used [23], where a transfer time of 5 ms was considered. Note, that the same dynamic model was used for all the discussed relay locations.

The developed model of a bi-directional overcurrent protection was verified with extensive laboratory testing using

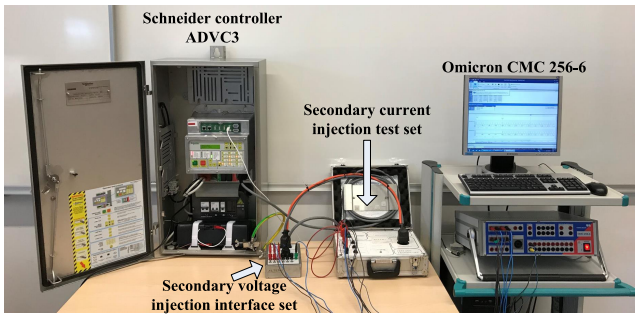

FIGURE 9. Laboratory set-up for secondary testing of a protection unit (Schneider controller ADVC3).

the set-up shown in Fig. 9. The test currents were varied within the range 1.2 to 5 times the pickup-current setting. The IEC extremely-inverse characteristic was tested, where $I_{Pj} = 500$ A and $T_{Dj} = 10$ ms. Time delays were determined for the model and for an actual protection unit as the difference between the measured operating times and the operating times obtained by (1). The time delays were shorter at higher currents for the protection model, as well as for an actual protection unit. The average value of the time delay was approximately 25 ms. However, the obtained time delay of the tested model and the actual unit were different within the acceptable range of ±5 ms. Moreover, the directional function was also tested for the proposed protection model and an actual protection unit.

VI. RESULTS

A. BEST OBJECTIVE FUNCTION VALUE AND CONVERGENCE

SADE was extensively tested for the case with the radial network topology. Self-adaptation was applied in two different ways, i.e., for the entire population, as well as for each population member. This is denoted as SADE1 and SADE2, respectively. Furthermore, ten different mutation strategies were considered. Table 6 shows the minimum, mean and standard deviations of the best values of the objective function q for 50 independent runs, where $\alpha = 0.3$, $\beta = 0.7$ and $t_{EV} = 0.3$ s. The convergence was also tested for the mutation strategies "rand/1/bin" and "rand/1/exp". Fig. 10 shows that for approximately the first 135 iterations the obtained values were penalized, whereas the minimum value was reached before 2500 iterations. The typical computation time for a single run of our implementation in Matlab on a 3-GHz Intel Core i5-7400 with 8 GB of RAM was less than 2 min. Furthermore, the results were also qualitatively the same for other network topologies, as well as when testing the objective function T. Based on the obtained results given in Table 6 and Fig. 10, the SADE1 variant and the "rand/1/bin" strategy were found to be the most suitable for the discussed optimization problem.

B. PICKUP-CURRENT LIMITS AND OCR SETTINGS

The obtained maximum-load currents $I_{j,L\,\max}$ and the minimum short-circuit currents $I_{j,SC\,\min}$ are shown in Fig. 11. Note

TABLE 6. Minimum, mean and standard deviation (Std. Dev.) of best q values for 50 independent runs – radial network topology.

	SADE1			SADE2		
Strategy	Min	Mean	Std. Dev.	Min	Mean	Std. Dev.
best/1/exp	1.051	1.144	0.117	1.033	1.117	0.069
rand/1/exp	1.028	1.039	0.003	1.023	1.038	0.009
rand-to-best/1/exp	1.024	1.057	0.042	1.029	1.053	0.025
best/2/exp	1.028	1.053	0.026	1.025	1.052	0.019
rand/2/exp	1.036	1.048	0.018	1.054	1.139	0.035
best/1/bin	1.034	1.187	0.131	1.027	1.133	0.083
rand/1/bin	1.018	1.021	0.004	1.018	1.027	0.005
rand-to-best/1/bin	1.027	1.059	0.084	1.021	1.056	0.016
best/2/bin	1.020	1.052	0.025	1.027	1.053	0.032
rand/2/bin	1.042	1.074	0.026	1.105	1.151	0.023

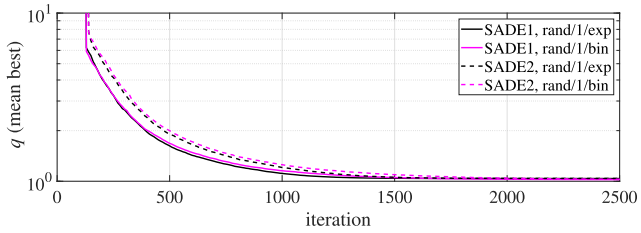

FIGURE 10. Mean best curves for 50 independent runs of selected algorithms – radial network topology.

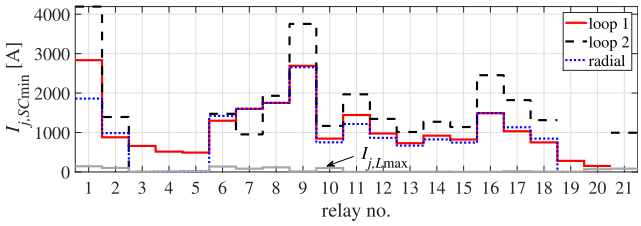

FIGURE 11. Maximum-load currents and minimum short-circuit currents for all three network topologies.

that equal values of $I_{j,L\,\max}$ were used for all three network topologies. The values $I_{j,SC\,\min}$ were determined according to the fault locations given in Table 4 and show considerable impacts of the network topology. Pickup-current limits were determined using (2), where $e_{CT\%} = 10\%$ and $K_{SC} = K_L = 1.1$ were considered. Furthermore, at several relays the value of $I_{j,L\,\max}$ is very small. In such cases $I_{Pj\,\min}$ was set to the estimated value of 50 A, which corresponds to a possible increase in demand over time.

The CTIs for the relay pairs between individual RSCs were 100 ms, while the CTIs for the relay pairs with substation relays R_1, R_6 and R_8 were 150 ms. Furthermore, the minimum time-dial setting was $T_{Dj\,\min} = 10$ ms. Minimization of the objective function (4), where $\alpha = 0.3$, $\beta = 0.7$, $t_{EV} = 0.3$ s, was performed using SADE1 and "rand/1/bin". The results are given in Table 7, where the obtained time-dial settings were rounded to 10 ms, whereas the obtained pickup-current settings were rounded to 1 A.

C. SELECTIVITY TESTING AND OPERATING TIMES

1) THEORETICAL CALCULATIONS

The operating times of the primary and back-up OCRs, i.e., $t_{(p,r)}$ and $t_{(b,r)}$, were calculated using (1) for the fault

TABLE 7. Relay settings – IEC Extremely Inverse ($A = 80$, $B = 2$, $C = 0$).

	Loop 1		Loop 2		Radial	
	I_{Pj} [A]	T_{Dj} [ms]	I_{Pj} [A]	T_{Dj} [ms]	I_{Pj} [A]	T_{Dj} [ms]
R_1	676	50	493	110	460	80
R_2	254	90	98	50	120	60
R_3	217	40	–	–	–	–
R_4	105	100	–	–	–	–
R_5	118	40	–	–	–	–
R_6	390	60	204	80	286	70
R_7	74	60	136	60	95	130
R_8	555	30	291	70	353	70
R_9	141	60	109	50	74	130
R_{10}	234	50	272	30	169	60
R_{11}	75	70	72	20	63	20
R_{12}	137	80	64	150	55	30
R_{13}	165	20	57	50	71	40
R_{14}	161	60	168	40	100	90
R_{15}	70	110	54	40	50	10
R_{16}	63	130	113	90	94	20
R_{17}	252	50	146	110	161	70
R_{18}	136	80	76	30	50	10
R_{19}	86	70	–	–	–	–
R_{20}	78	10	–	–	–	–
R_{21}	–	–	91	100	–	–

TABLE 8. Operating times of substation OCRs for a fault at the beginning of a feeder.

		Loop 1 $t^*_{j,k}$ [ms]	Loop 2 $t^*_{j,k}$ [ms]	Radial $t^*_{j,k}$ [ms]
R_1	FL_1	70	80	51
R_6	FL_{10}	28	10	18
R_8	FL_{13}	28	18	26

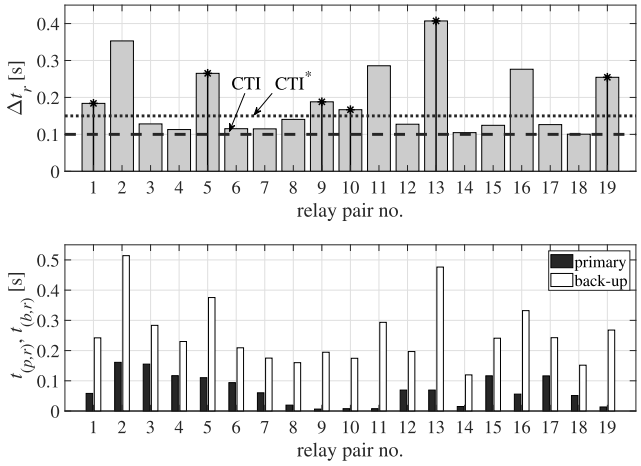

FIGURE 12. Δt_r values and operating times of primary and back-up OCRs – Loop-1 topology, where (·)* denotes the relay pairs with substation OCRs.

locations given in Table 2, while using the optimum settings. The results are shown in Figs. 12–14, together with the Δt_r values. Note that the results denoted as $(\cdot)^*$ are given for relay pairs with substation OCRs (R_1, R_6 and R_8). Selectivity is achieved for all the relay pairs since $\Delta t_r > \text{CTI}_r$. Moreover, selectivity is also assured for the substation OCRs, since $t^*_{j,k} < 300$ ms, as is shown in Table 8.

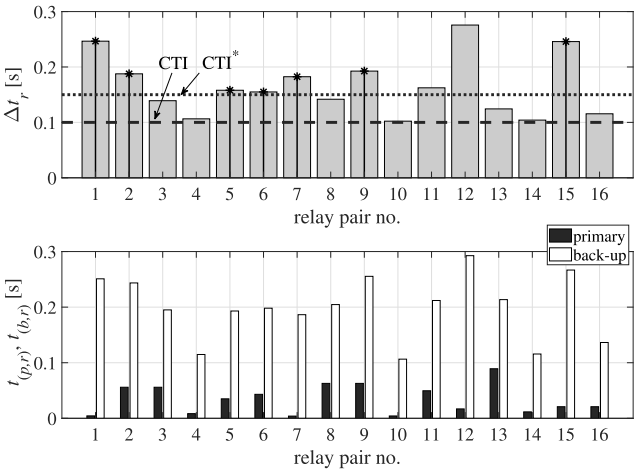

FIGURE 13. Δt_r values and operating times of primary and back-up OCRs – Loop-2 topology, where (·)* denotes the relay pairs with substation OCRs.

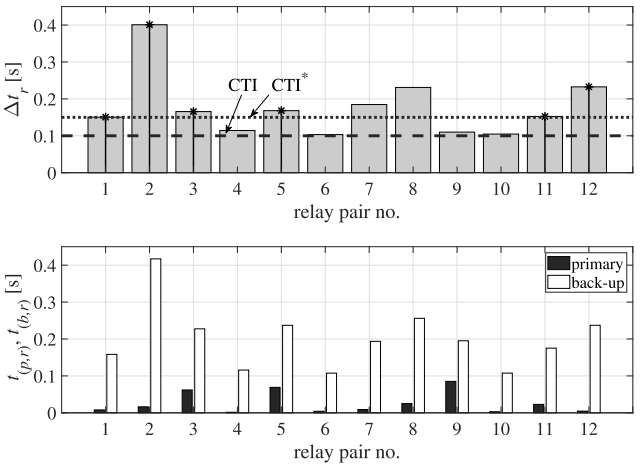

FIGURE 14. Δt_r values and operating times of primary and back-up OCRs – Radial topology, where (·)* denotes the relay pairs with substation OCRs.

2) DYNAMIC SIMULATIONS

The models proposed in Section V-B were used, while using the optimum settings given in Table 7. The Ph-Ph faults were simulated for all possible fault locations. The simulations were performed for the RSCs with and without the GOOSE communications. The resulting clearing times are given in Table 9, which include the operation of the RSCs (relay and switch gear), as well as the 5-ms transfer time in the case of the communications. The RSCs without communications operated in a selective way according to the expected time delays. Furthermore, faults located close to the substation cannot be picked-up with in-loop RSCs, e.g., for the Loop-1 topology the R_{20} does not pick-up for a fault at FL_1. Consequently, the R_1 operated first, which increased the current through the R_{20} that was then picked-up. The same situation was observed for the fault at FL_{10} and the operation

TABLE 9. Results of dynamic simulations for all the fault locations and all the topologies, where the clearing times include the operation of the RSCs (relay and switch gear) and communication transfer times.

	Loop 1			Loop 2			Radial		
	operated	without comm. $t_{j,k}$ [ms]	with comm. $t_{j,k}$ [ms]	operated	without comm. $t_{j,k}$ [ms]	with comm. $t_{j,k}$ [ms]	operated	without comm. $t_{j,k}$ [ms]	with comm. $t_{j,k}$ [ms]
FL_1	R_1 & R_{20}	134, 213	134, 213	R_1	134	74	R_1	114	74
FL_2	R_1 & R_{20}	273, 124	72, 72	R_1	302	73	R_1	213	73
FL_3	R_2 & R_{19}	114, 210	72, 72	R_2	63	63	R_2	63	63
FL_4	R_2 & R_{19}	542, 137	62, 61	R_2	92	71	R_2	131	71
FL_5	R_3 & R_{18}	267, 281	69, 66	R_{18}	81	81	R_{18}	63	63
FL_6	R_3 & R_{18}	343, 175	73, 71	R_{18}	61	61	R_{18}	61	61
FL_7	R_4 & R_{17}	271, 311	62, 62	R_{17}	171	71	R_{17}	173	73
FL_8	R_4 & R_{17}	280, 191	69, 65	R_{17}	113	73	R_{17}	123	72
FL_9	R_5 & R_6	235, 352	62, 62	R_6 & R_7	201, 233	73, 64	R_7	212	72
FL_{10}	R_5 & R_6	352, 83	352, 83	R_6 & R_7	64, 193	64, 193	R_6	74	65
FL_{11}	R_7	63	63	R_6 & R_7	143, 94	73, 64	R_7	83	83
FL_{12}	R_8	252	73	R_8 & R_{21}	153, 104	64, 69	R_8	183	73
FL_{13}	R_8	94	74	R_8 & R_{21}	74, 191	74, 191	R_8	74	66
FL_{14}	R_9	63	63	R_9	63	63	R_9	63	63
FL_{15}	R_9	73	73	R_9	63	63	R_9	63	63
FL_{16}	R_{16}	72	72	R_{16}	82	82	R_{16}	62	62
FL_{17}	R_{16}	72	72	R_{16}	92	92	R_{16}	62	62
FL_{18}	R_5 & R_6	255, 371	61, 62	R_6 & R_7	204, 243	73, 64	R_7	221	72
FL_{19}	R_{10}	122	72	R_{10}	122	72	R_{10}	122	72
FL_{20}	R_{11}	71	71	R_{11}	61	61	R_{11}	63	63
FL_{21}	R_{12}	181	181	R_{12}	111	111	R_{12}	71	71
FL_{22}	R_{12}	191	191	R_{12}	112	112	R_{12}	71	71
FL_{23}	R_{15}	111	111	R_{15}	71	71	R_{15}	61	61
FL_{24}	R_{15}	123	123	R_{15}	74	74	R_{15}	61	61
FL_{25}	R_{13}	151	151	R_{13}	81	81	R_{13}	101	101
FL_{26}	R_{13}	111	111	R_{13}	71	71	R_{13}	83	83
FL_{27}	R_{14}	181	71	R_{14}	151	73	R_{14}	141	71
FL_{28}	R_{11}	71	71	R_{11}	61	61	R_{11}	61	61
FL_{29}	R_7	71	71	R_6 & R_7	114, 131	73, 64	R_7	93	93

FIGURE 15. Photographs of Ph-Ph faults due to falling trees.

of R_5 and R_6. Obviously, communications could not be activated for the discussed fault locations FL_1 and FL_{10}, which was confirmed with the obtained results. A similar result was also noticed for the Loop-2 topology for the fault locations FL_{10} and FL_{13}. Based on the obtained results it can be concluded that the operating times of the communication-assisted RSCs were significantly reduced.

D. IMPLEMENTATION

The proposed protection design is already implemented in a 20-kV network of DisCo Elektro Celje using compact RSCs. Even though the GOOSE communications are not yet established, the field results are promising. During two recent Ph-Ph faults in the section between R_3 and R_{18} (Loop 1) and one Ph-Ph fault in the end branch near R_{15} the protection operated in a reliable and selective way. Fig. 15 shows photographs of the discussed Ph-Ph faults that were all on overhead lines due to falling trees. Note that before modernization, the discussed network operated in a radial arrangement of feeders, using only the substation relays R_1, R_6 and R_8. Consequently, these Ph-Ph faults would have resulted in an outage of 2124 customers. However, according to the data

obtained from DisCo Elektro Celje, only 49 customers were out of power during faults in the section between R_3 and R_{18}, while for a fault in the end branch near R_{15} only 26 customers were disconnected. It should be emphasized, that the resulting operation of the RSCs is due to the closed-loop operation and an appropriate protection design.

VII. CONCLUSION

This paper proposes measures that improve the operation of OCRs in MV closed-loop distribution networks. The selectivity of the substation OCRs is achieved by considering the required maximum operating time (300 ms), while the unwanted trips of the in-loop OCRs are avoided by a simple procedure for short-circuit calculations. The proposed timing coordination of the OCRs' operation minimizes the operating times and increases the sensitivity of all the relays, i.e., RSCs and substation OCRs. Preliminary results showed that, when using the classic DE in combination with fixed penalties, the optimization process was not converging for the discussed case study. Therefore, variable penalties were introduced that force the optimization procedure towards the region with the viable solutions of the optimization problem. Furthermore, SADE was used, which showed considerably better convergence than the classic DE. Two variants of SADE were extensively tested together with ten mutation strategies. Based on the obtained results the strategy "rand/1/bin" was chosen together with a SADE variant that is based on the self-adaptation of the control parameters for the entire population. The resulting operating times of the OCRs are comparable with the operating times determined using methods known in the literature. Moreover, adopting the GOOSE communications reduces the operating times, which was fully confirmed through the dynamic simulations of the Ph-Ph faults in the discussed 20-kV network. The discussed protection design with compact RSCs is already implemented and operates permanently in a 20-kV network of DisCo Elektro Celje that supplies more than 5000 customers. Field results are promising; even though the GOOSE communications are not yet established, the RSCs have selectively operated during recent Ph-Ph faults. Thus, we can expect that the SAIDI and SAIFI will be improved in the future. There are natural extensions for the work presented in this paper, especially the adaptation of the proposed measures for the improved operation of ground fault-protection relays in MV closed-loop distribution networks.

REFERENCES

[1] D. P. Le, D. M. Bui, C. Ngo, and A. Le, "FLISR approach for smart distribution networks using E-terra software—A case study," *Energies*, vol. 11, no. 12, Dec. 2018, Art. no. 3333.

[2] *Definitions for Power Switchgear*, IEEE Standard C37.100-1992 (R2001), 2001.

[3] J. Sykes, "Reliability fundamentals of system protection," NERC, Princeton, NJ, USA, NERC SPCS Rep., 2010. [Online]. Available: https://www.nerc.com/comm/PC/Pages/System%20Protection%20and%20Control%20Subcommittee%20(SPCS)/System-Protection-and-Control-Subcommittee-SPCS.aspx

[4] A. S. Noghabi, H. R. Mashhadi, and J. Sadeh, "Optimal coordination of directional overcurrent relays considering different network topologies using interval linear programming," *IEEE Trans. Power Del.*, vol. 25, no. 3, pp. 1348–1354, Jul. 2010.

[5] T. Amraee, "Coordination of directional overcurrent relays using seeker algorithm," *IEEE Trans. Power Del.*, vol. 27, no. 3, pp. 1415–1422, Jul. 2012.

[6] V. A. Papaspiliotopoulos, G. N. Korres, and N. G. Maratos, "A novel quadratically constrained quadratic programming method for optimal coordination of directional overcurrent relays," *IEEE Trans. Power Del.*, vol. 32, no. 1, pp. 3–10, Feb. 2017.

[7] D. L. A. Negrão and J. C. M. Vieira, "The local fit method for coordinating directional overcurrent relays," *IEEE Trans. Power Del.*, vol. 31, no. 4, pp. 1464–1472, Aug. 2016.

[8] M. Y. Shih, A. C. Enríquez, T.-Y. Hsiao, and L. M. T. Treviño, "Enhanced differential evolution algorithm for coordination of directional overcurrent relays," *Elect. Power Syst. Res.*, vol. 143, pp. 365–375, Feb. 2017.

[9] M. H. Costa, R. R. Saldanha, M. G. Ravetti, and E. G. Carrano, "Robust coordination of directional overcurrent relays using a matheuristic algorithm," *IET Gener., Transmiss. Distrib.*, vol. 11, no. 2, pp. 464–474, 2017.

[10] F. Razavi, H. A. Abyaneh, M. Al-Dabbagh, R. Mohammadi, and H. Torkaman, "A new comprehensive genetic algorithm method for optimal overcurrent relays coordination," *Elect. Power Syst. Res.*, vol. 78, pp. 713–720, Apr. 2008.

[11] F. B. Bottura, W. M. S. Bernardes, M. Oleskovicz, and E. N. Asada, "Setting directional overcurrent protection parameters using hybrid GA optimizer," *Elect. Power Syst. Res.*, vol. 143, pp. 400–408, Feb. 2017.

[12] A. A. Kida and L. A. Gallego, "A high-performance hybrid algorithm to solve the optimal coordination of overcurrent relays in radial distribution networks considering several curve shapes," *Elect. Power Syst. Res.*, vol. 140, pp. 464–472, Nov. 2016.

[13] D. Saha, A. Datta, and P. Das, "Optimal coordination of directional overcurrent relays in power systems using symbiotic organism search optimisation technique," *IET Gener., Transmiss. Distrib.*, vol. 10, no. 11, pp. 2681–2688, May 2016.

[14] M. Singh, B. K. Panigrahi, and A. R. Abhyankar, "Optimal coordination of directional over-current relays using teaching learning-based optimization (TLBO) algorithm," *Int. J. Elect. Power Energy Syst.*, vol. 50, pp. 33–41, Sep. 2013.

[15] H. H. Zeineldin, E. F. El-Saadany, and M. M. A. Salama, "Optimal coordination of overcurrent relays using a modified particle swarm optimization," *Electr. Power Syst. Res.*, vol. 76, no. 11, pp. 988–995, 2006.

[16] M. Y. Shih, C. A. C. Salazar, and A. C. Enríquez, "Adaptive directional overcurrent relay coordination using ant colony optimisation," *IET Gener., Transmiss. Distrib.*, vol. 9, no. 14, pp. 2040–2049, Nov. 2015.

[17] A. Wadood, T. Khurshaid, S. G. Farkoush, J. Yu, C.-H. Kim, and S.-B. Rhee, "Nature-inspired whale optimization algorithm for optimal coordination of directional overcurrent relays in power systems," *Energies*, vol. 12, no. 12, Jun. 2019, Art. no. 229.

[18] H. H. Zeineldin, H. M. Sharaf, D. K. Ibrahim, and E. E.-D. A. El-Zahab, "Optimal protection coordination for meshed distribution systems with DG using dual setting directional over-current relays," *IEEE Trans. Smart Grid*, vol. 6, no. 1, pp. 115–123, Jan. 2015.

[19] L. Huchel and H. H. Zeineldin, "Planning the coordination of directional overcurrent relays for distribution systems considering DG," *IEEE Trans. Smart Grid*, vol. 7, no. 3, pp. 1642–1649, May 2016.

[20] K. Pereira, B. R. Pereira, J. Contreras, and J. R. S. Mantovani, "A multiobjective optimization technique to develop protection systems of distribution networks with distributed generation," *IEEE Trans. Power Syst.*, vol. 33, no. 6, pp. 7064–7075, Nov. 2018.

[21] S. Katyara, L. Staszewski, and Z. Leonowicz, "Protection coordination of properly sized and placed distributed generations-methods, applications and future scope," *Energies*, vol. 11, no. 10, Oct. 2018, Art. no. 2627.

[22] *Communication Networks and Systems for Power Utility Automation, 2.0*, Standard IEC 61850, 2013.

[23] A. Apostolov, "To GOOSE or not to GOOSE?—That is the question," in *Proc. 68th Annu. Conf. Protective Relay Eng.*, College Station, TX, USA, 2015, pp. 583–596.

[24] Y. Liu, H. Gao, W. Gao, and F. Peng, "Development of a substation-area backup protective relay for smart substation," *IEEE Trans. Smart Grid*, vol. 8, no. 6, pp. 2544–2553, Nov. 2017.

[25] S. Kumar, N. Das, and S. Islam, "High voltage substation automation and protection system based on IEC 61850," in *Proc. AUPEC*, Auckland, New Zealand, 2018, pp. 1–6.
[26] M. A. Aftab, S. Roostaee, S. M. S. Hussain, I. Ali, M. S. Thomas, and S. Mehfuz, "Performance evaluation of IEC 61850 GOOSE-based inter-substation communication for accelerated distance protection scheme," *IET Gener., Transmiss. Distrib.*, vol. 12, no. 18, pp. 4089–4098, Oct. 2018.
[27] A. Leal and J. F. Botero, "Defining a reliable network topology in software-defined power substations," *IEEE Access*, vol. 7, pp. 14323–14339, Feb. 2019.
[28] S. M. Farooq, S. M. S. Hussain, and T. S. Ustun, "Performance evaluation and analysis of IEC 62351-6 probabilistic signature scheme for securing GOOSE messages," *IEEE Access*, vol. 7, pp. 32343–32351, 2019.
[29] J. Brest, S. Greiner, B. Boskovic, M. Mernik, and V. Zumer, "Self-adapting control parameters in differential evolution: A comparative study on numerical benchmark problems," *IEEE Trans. Evol. Comput.*, vol. 10, no. 6, pp. 646–657, Dec. 2006.
[30] K. Price, R. M. Storn, and J. A. Lampinen, *Differential Evolution: A Practical Approach to Global Optimization*. Berlin, Germany: Springer-Verlag, 2005.
[31] M. Ojaghi and R. Ghahremani, "Piece-wise linear characteristic for coordinating numerical overcurrent relays," *IEEE Trans. Power Del.*, vol. 32, no. 1, pp. 145–151, Feb. 2017.
[32] *Measuring Relays and Protection Equipment—Part 151: Functional Requirements of Over/Under Current Protection*, Standard IEC 60255-151, 2009.
[33] *Inverse-Time Characteristics Equations for Overcurrent Relays*, IEEE Standard C37.112-2018, 2018.
[34] *Guide for Protective Relay Applications to Distribution Lines*, IEEE Standard C37.230-2007, 2007.
[35] V. C. Nikolaidis, E. Papanikolaou, and A. S. Safigianni, "A communication-assisted overcurrent protection scheme for radial distribution systems with distributed generation," *IEEE Trans. Smart Grid*, vol. 7, no. 1, pp. 114–123, Jan. 2016.
[36] *ADVC Controller Range Operations Manual, R29*, Schneider Electr., Brisbane, QLD, Australia, 2018.

BOŠTJAN POLAJŽER (M'13) received the B.Sc. and Ph.D. degrees in electrical engineering from the Faculty of Electrical Engineering and Computer Science, University of Maribor, Maribor, Slovenia, in 1997 and 2002, respectively. Since 1998, he has been with the Faculty of Electrical Engineering and Computer Science, University of Maribor, where he has been an Associate Professor, since 2010. In 2000, he was a Visiting Scholar with the Catholic University Leuven, Leuven, Belgium, and the Graz University of Technology, Graz, Austria, in 2019. His research interests include electrical machines and devices, power quality, and power-system protection and control.

MATEJ PINTARIČ received the M.Eng. degree in electrical engineering from the Faculty of Electrical Engineering and Computer Science, University of Maribor, Maribor, Slovenia, in 2016. Since 2016, he has been an Assistant of electrical engineering with the Faculty of Electrical Engineering and Computer Science, University of Maribor. His research interests include smart grids and energy management.

MIRAN ROŠER received the degree from the Department of FERI, Technical Faculty, University of Maribor, in 2004, and the Ph.D. degree from the Faculty of Electrical Engineering, Computer Science and Informatics, Maribor, in 2014. He is currently an Employee with Elektro Celje, d. d., where he deals with measurements and relay protection systems as well as methods for managing and analyzing the operation and development of the distribution networks. He also deals with the implementation of modern solutions within the framework of smart-grid projects.

GORAZD ŠTUMBERGER (M'92) received the B.Sc., M.Sc., and Ph.D. degrees from the University of Maribor, Maribor, Slovenia, in 1989, 1992, and 1996, respectively, all in electrical engineering. Since 1989, he has been with the Faculty of Electrical Engineering and Computer Science, University of Maribor, where he is currently a Professor of electrical engineering. In 1997 and 2001, he was a Visiting Researcher with the University of Wisconsin, Madison, and with the Catholic University Leuven, Leuven, Belgium, in 1998 and 1999. His current research interests include power-system research and the design, modeling, analysis, and control of electrical machines and drives.